



Published in final edited form as:

Bioconjug Chem. 2015 June 17; 26(6): 963–974. doi:10.1021/acs.bioconjchem.5b00167.

Molecular Probes for Fluorescence Lifetime Imaging

Pinaki Sarder¹, Dolonchampa Maji^{1,2}, and Samuel Achilefu^{1,2,3,*}

¹Department of Radiology, Washington University School of Medicine, 4525 Scott Avenue, St. Louis, Missouri 63110

²Department of Biomedical Engineering, Washington University School of Medicine, 4525 Scott Avenue, St. Louis, Missouri 63110

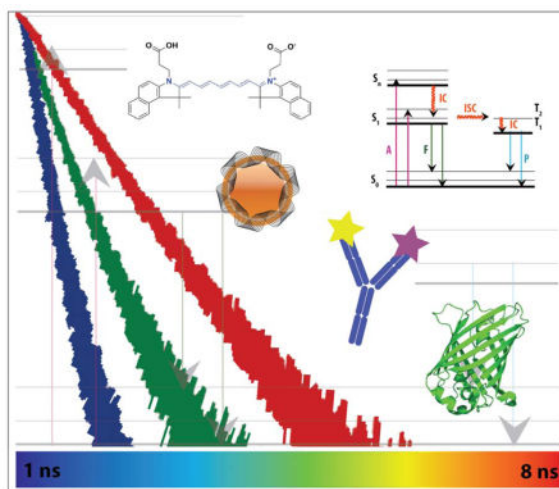
³Department of Biochemistry and Molecular Biophysics, Washington University School of Medicine, 4525 Scott Avenue, St. Louis, Missouri 63110

Abstract

Visualization of biological processes and pathologic conditions at the cellular and tissue levels largely rely on the use of fluorescence intensity signals from fluorophores or their bioconjugates. To overcome the concentration dependency of intensity measurements, evaluate subtle molecular interactions, and determine biochemical status of intracellular or extracellular microenvironments, fluorescence lifetime (FLT) imaging has emerged as a reliable imaging method complementary to intensity measurements. Driven by a wide variety of dyes exhibiting stable or environment-responsive FLTs, information multiplexing can be readily accomplished without the need for ratiometric spectral imaging. With knowledge of the fluorescent states of the molecules, it is entirely possible to predict the functional status of biomolecules or microenvironment of cells. Whereas the use of FLT spectroscopy and microscopy in biological studies is now well established, *in vivo* imaging of biological processes based on FLT imaging techniques is still evolving. This review summarizes recent advances in the application of the FLT of molecular probes for imaging cells and small animal models of human diseases. It also highlights some challenges that continue to limit the full realization of the potential of using FLT molecular probes to address diverse biological problems, and outlines areas of potential high impact in the future.

*Correspondence: Samuel Achilefu, PhD, Department of Radiology, Washington University School of Medicine, 4525 Scott Avenue, St. Louis, MO 63110, Tel: 314-362-8599, achilefus@mir.wustl.edu.

The authors declare no competing financial interest.



1. INTRODUCTION

Singlet state fluorescence occurs when a fluorophore absorbs radiation of specific energy, followed by the emission of photons as the molecule returns to the ground state. Because energy is lost between the excitation and emission processes, fluorescence is emitted at a higher wavelengths than those of the excitation radiation.¹ Several factors affect molecular fluorescence, including the molecular structures and associated vibrational energy levels, as well as the physical and chemical environment of the fluorophores.^{1, 2} Perturbation of the fluorescence of many organic molecules could decrease the quantum yield at the same emission wavelength or cause spectral shift. Both effects are useful for biological applications. Within linearity, changes in the fluorescence intensity can be used to determine the concentration of fluorophores in a medium. Shifts in the spectral profile of fluorophores can provide quantitative data *via* ratiometric measurements at two different wavelengths. Although these approaches are highly reliable for reporting biological events in solutions or shallow surfaces, enhanced light scattering and absorption in heterogeneous mediums such as cells and tissue can adversely affect the fluorescence intensity in a less predictable manner. For these reasons, most fluorescence measurements in cells and tissue are typically reported in a relative intensity measurement using calibration standards or by self-referencing.

Unlike fluorescence intensity-based imaging, fluorescence lifetime (FLT) of molecular probes is less dependent on the local fluorophore concentration or the method of measurement, which minimizes imaging artifacts and provides reproducible quantitative measurements over time.¹ The FLT of fluorophores is the average time a molecule spends in the excited state between absorption and emission of radiation before returning to the ground state.¹ Accurate determination of the FLT of fluorophores and application in biological imaging and spectroscopy depend on both instrumentation and understanding of the fluorophore system. The FLT of a fluorophore can be measured by spectroscopic, microscopic, or *in vivo* imaging methods. Several FLT instruments are commercially available for spectroscopic and microscopic FLT measurements. For *in vivo* imaging, many studies rely on custom-built FLT systems³ because the only company (ART – Advanced

Research Technologies, Canada) producing a commercial system is no longer operational. Because several papers have reviewed advances in FLT measurement methods and devices, this review will focus on fluorophore systems and how changes in their FLT contribute to our understanding of biological events. FLT of a molecule changes with small changes in the immediate microenvironment of the molecules, and therefore can be used to report cellular and molecular processes with very high sensitivity.¹

Classification of molecular probes used for FLT imaging can be based on their FLT properties, emission wavelengths, or response to specific biological microenvironment.⁴ Figure 1 shows some fluorophore systems commonly used for lifetime imaging and the range of their photoluminescence lifetimes. To simplify this review article, we have broadly narrowed the types of molecular probes used in FLT imaging into endogenous and exogenous imaging agents. Our discussion of the exogenous agents is grouped into stable, as well as chemical and physical environment responsive FLT fluorophore systems. Our discussion primarily focuses on singlet state fluorescence.

2. ENDOGENOUS FLT FLUOROPHORES

Most biospecimens possess intrinsic fluorescence because of the presence of some fluorescent biomolecules such as aromatic amino acids, fluorescent pigments, reduced nicotinamide adenine dinucleotide (NADH), flavin adenine dinucleotide (FAD), porphyrin, and some structural proteins.⁵ The expression levels or locations of these biomolecules can inform investigators on the functional status of cells and tissue. Several studies have utilized FLT imaging to differentiate healthy from diseased tissue. Examples include atherosclerotic plaques^{6, 7} and various types of tumors.^{8–10} Below is a summary of the application of the most commonly reported endogenous fluorophores in FLT imaging.

2.1. Melanin

Melanin (ex/em: 340–400/360–560 nm) is a pigment produced by melanocytes and widely present in living organisms.¹¹ FLT of melanin range up to ~8 ns.⁵ Current literature has focused on studying FLT of melanin in healthy and cancerous skin. Studies have shown that the FLT of melanin can discriminate between healthy skin and basal cell carcinoma (BCC), as well as melanoma in fresh biopsies.^{12, 13} Another work demonstrated a significant difference in FLT between keratinocytes and melanocytes, information that was used to characterize melanoma.¹⁴ FLT of melanin has also been used as the baseline indicator for detecting oxidative stress conditions in retinal pigment epithelial cells.¹⁵ With the miniaturization of FLT systems, it is expected that FLT measurements can be used to screen suspicious lesions at point-of-care settings in the future.

2.2. NAD(P)H/FAD

NADH and its phosphate derivative NADPH (ex/em: 350/450 nm) are the dominant endogenous fluorophores in cells participating in cell metabolism, reductive biosynthesis, antioxidation, cell signaling, aging, and regulation of apoptosis.¹⁶ They have a mean FLT ~2.3–3.0 ns when bound to proteins and a short FLT ~0.3–0.4 ns in free form.⁵ Their FLTs are sensitive to solvent polarity and viscosity, and are affected by their dynamic quenching

in the presence of adenine moiety.^{17, 18} FAD is another endogenous fluorophore that plays the role of redox cofactor in cells. FAD emits at a longer wavelength (ex/em: 450/535 nm) than NAD(P)H. Only the unbound form of FAD is fluorescent, with an FLT of 2.3–2.9 ns.⁵ The complementary metabolic functions of FAD and NAD(P)H allow the use of their FLT changes to report the metabolic state of cells. Physiologic parameters such as pH and O₂ levels, as well as changes in tyrosine or tryptophan concentrations and local temperature are readily obtained from NAD(P)H/FAD FLT measurements.¹⁹

FLT of NADH has been extensively studied in early detection and diagnosis of skin cancer. A recent study reported measuring the FLT of NADH at different depths from the tissue surface in fresh biopsies of both healthy skin and BCC. Different mean FLTs ranging from 800 to 950 ps were measured along different healthy skin layers. This is attributable to differences in the metabolic state of different layers of healthy tissue. In contrast, negligible variation of FLT was observed in BCC skin layers because BCC is characterized by hyperproliferation of basal cells inside the epidermis, obviating the cellular differentiation typical of healthy skin.²⁰ The inverse relationship between the FLT of protein-bound FAD and NAD concentration (a non-fluorescent oxidized form of NADH) has been used to determine NAD level in cells.²¹ In a recent clinical investigation, diffuse reflectance and time-resolved autofluorescence spectra of skin was used to correctly diagnose 87% of the BCCs in 25 patients.²² Another clinical study described a significant difference between the mean average autofluorescence (including contribution from NADH) lifetimes (570 ± 740 ps) using 47 endoscopic specimen of normal and neoplastic (adenomatous polyp) excision biopsy/resection samples from colon.²³

Imaging of brain activity has become an exciting field of research because of the potential to predict a variety of neurological diseases *via* imaging. In optical imaging, absorption mode is currently used to map brain activity, but this method relies heavily on subtle changes in the ratio of oxy- and deoxy-hemoglobin. To improve detection sensitivity, the FAD/NAD(P)H fluorescence ratio can be used for determining changes in cellular metabolism during neuronal activity. However, FLT measurements may provide more stable longitudinal data in high throughput format by measuring the FLT of either NAD(P)H or FAD at a single wavelength.^{8, 24} This information can then be correlated with other factors without the need to measure multiple FLTs. NADH and FAD lifetimes have also been employed to accurately distinguish healthy hearts from diseased hearts with infarcted myocardium in rat models.²⁵

3. EXOGENOUS FLUOROPHORES

The shallow penetration of light in the ultraviolet and visible light regions of the electromagnetic spectrum, as well as the low expression of a target endogenous fluorophores in tissues of interest confines the applications of these measurements to specialized cases of pathophysiology. In addition, the weak and nonspecific nature of the endogenous fluorescence further requires long signal acquisition time and sophisticated image analysis software to enhance detection sensitivity and decipher different types of tissue. These limitations can be overcome by the use of exogenous contrast agents.⁴

The FLT of some fluorophores are minimally affected under diverse biologically relevant conditions. These molecules provide stable FLT imaging data in different tissues. In many cases, the local environment can alter the FLT of other fluorophores. To achieve specific response, changes in FLT can be induced through diverse molecular designs. Selective delivery of many fluorescent molecules to target cells or intracellular compartments is typically achieved by conjugating the fluorophores to biomolecules. Depending on the fluorophore, conjugation can retain or alter the FLT of the dye. A recent study showed that conjugation of rhodamine derivatives to amine dendrimers altered the FLT based on the ratio of dye to dendrimer.²⁶ This provides a simple method to determine the number of substituents per dendrimer, and could be used to distinguish free versus covalently bound dye molecules. We highlight these different molecular imaging strategies below based on the FLT of fluorophores.

3.1. Static FLT Probes

Fluorescent molecular probes and nanoparticles that do not exhibit significant changes in their FLT in biological medium are static FLT probes. Stability of the FLT provides reliable imaging signal over time and can be used to improve the spatial resolution of the molecular probe distribution without distortion from intractable FLT in different compartments. For example, the stable FLT of fluorescent nanodiamonds, which is distinct from tissue autofluorescence FLT, was successfully used to track lung stem cells *in vivo*.²⁷ Static FLT molecular probes are particularly useful in information multiplexing. By targeting different biomolecules with molecular probes exhibiting different FLT, quantitative ratio-imaging can readily be achieved without compensating for imaging artifacts encountered in intensity-based measurements. A unique feature of this approach is the potential to image fluorophores with similar excitation and emission wavelengths, but with different FLT (Figure 2).²⁸ This capability overcomes wavelength-dependent attenuation of light in tissue, which affects fluorescence intensity readouts. Furthermore, the limited number of emission channels in regular confocal microscopes or *in vivo* imaging systems limits the scope of intensity-based multiplexed imaging or cell sorting. In contrast, it is possible to track different types of cells labeled with fluorescent dyes of distinct FLT in small animals or in culture to understand disease pathology.^{28, 29}

3.2. Responsive FLT Molecular Probes

Unlike stable FLT molecular probes, the need to quantitatively interrogate molecular processes without resorting to ratiometric imaging techniques has stimulated the design of reporter molecules that change FLT as a function of their environment. These designs utilize similar approaches used to develop intensity-based activatable molecular probes.³⁰ We have classified these FLT imaging agents on the basis of the response mechanism – biomolecular, biochemical, and biophysical.

3.2.1. Biomolecular Binding-Responsive FLT Molecular Probes—Many fluorescent probes are designed to alter their FLT in response to biological events. Förster resonance energy transfer (FRET) technique is particularly useful for reporting molecular interactions *in vitro* and *in vivo*. Adjacent fluorophores can perturb the residence time of fluorescent molecules in the excited state, leading to a decrease in the average residence

time in this state. Although FLT is less dependent on fluorophore concentration, detectable fluorescence signal is still required to measure this parameter. In molecular designs where the fluorescence is completely quenched, FLT imaging would resemble traditional fluorescence enhancement *via* activatable probe method. However, instead of reporting increase in fluorescence intensity, a well calibrated FLT decrease relative to the distance of the quenching or acceptor molecule could be used to determine distance-dependent molecular interactions with high accuracy. Here, energy transfer from a fluorescent donor to an acceptor molecule is expected to decrease the donor FLT. In this section, we discuss FRET-based studies that alter FLTs through biologically-induced disruption of interaction between the acceptor and donor fluorescent molecules.

FLTs of fluorescent proteins (0.1–4 ns) used to design donor-acceptor FRET pairs provide excellent FLT maps of biomolecular interactions or activities by fluorescence lifetime imaging microscopy (FLIM). Examples of fluorescent protein pairs for FRET-based FLIM include green fluorescent protein (GFP)–DsRed (ex/em: 395/509–554/586 nm),³¹ GFP–mCherry (ex/em: 395/509–587/610 nm),³² cyan fluorescent protein (CFP)–Venus (ex/em: 435/485–515/528 nm),³³ and CFP–yellow fluorescent protein (YFP) (ex/em: 435/485–514/527 nm).³⁴ Small organic dyes (FLT: 0.1–90 ns) that undergo FRET are also used for FRET-based FLIM. Examples of such pairs include Alexa Fluor (AF) 488–Cy3 (ex/em: 495/519–550/570 nm),³⁵ AF488–AF647 (ex/em: 495/519–650/665 nm),³⁶ Cy3–Cy5 (ex/em: 550/570–650/670 nm),³⁷ and AF700–AF750 (ex/em: 702/723–749/775 nm).³⁸ Lanthanides paired with organic dyes³⁹ or with fluorescent proteins,⁴⁰ have also been used as FRET donors because of their stable and long FLTs (μ s to ms).⁴ FRET-based techniques using FLT measurements are perhaps the most widely used approach to image molecular interactions in cells. Recent comprehensive review articles on FLT-based FRET studies are available.^{4, 41} To maintain the concise nature of this review, we have confined our examples to representative citation for each application described below.

FRET-based FLT molecular designs have been used to report the activity of enzymes, such as proteases. This approach is particularly useful for endoproteases, where the amide cleavage site is flanked by several amino acids, allowing the incorporation of donor-acceptor fluorescent molecules at both ends of a peptide substrate without disrupting the enzyme activity. Examples include imaging the use of caspase-3 FRET-FLT substrate to image the up-regulation of caspase-3 in cancer.⁴² Similarly, a FRET pair consisting of fluorescein (ex/em: 494/521 nm; donor)-bovine serum albumin (BSA; acceptor) conjugate was used to determine intracellular proteolysis of BSA *via* FLT increase from 0.5 to 3.0 ns.⁴³

Instead of using dynamic donor-acceptor fluorophore quenching for FRET, some investigators prefer static quenching using macro-molecular self-quenched probe designs. Here, multiple fluorescent molecules are linked to a polymeric or large molecule to alter the absorption and, most often, quench the dye fluorescence. By using FLT instead of intensity measurement, high fluorescence quenching, which could affect enzyme recognition of the substrate, is not necessary. A change in FLT from the initial value will then be used to track biological activity. Recently, Goergen *et al.*⁴⁴ synthesized cathepsin B activatable macromolecular probe using IRDye 800CW (ex/em: 778/794 nm). Spectroscopic analysis showed FLT increase upon cleavage of specific amide bonds by cathepsin B. *In vivo* FLT

imaging of cathepsin B activity in mouse infarcted myocardium was achieved with the molecular probe. FLT imaging was able to distinguish nonspecifically accumulated molecular probe in the liver from the cathepsin B activated reporter system in the infarcted regions.⁴⁴ A similar study by Solomon *et al.* employed a self-quenched enzyme cleavable FRET probe, MMPSense750 FAST (ex/em: 749/775 nm), for imaging the expression of matrix metalloproteinases in tumor bearing mice.⁴⁵ Alford *et al.* further demonstrated the versatility of this FLT approach by conjugating trastuzumab (which targets human epidermal growth factor receptor 2 (HER2/neu) receptor) with AF750 (ex/em: 749/775 nm).⁴⁶ Digestion of the antibody upon cellular internalization released the dye molecules, leading to predictable FLT increase.⁴⁶

Conjugation of some molecular probes with biomolecules can alter their FLT, which can be used to determine successful conjugation and molecular interactions. For example, the glucose sensor, Badan (ex/em: 400/550 nm), has a low FLT (~0.8 ns) in the native form, but it increases to ~3.1 ns when bound to glucose.⁴⁷ Similarly, conjugation of Cy5.5 (ex/em: 673/707 ns) with an antibody targeted to human CD20 antigen for studying B-cell malignancies⁴⁸ exhibited variable FLTs in the tumor core (1.83–1.93 ns) and periphery (1.7–1.75 ns). Ardeshirpour *et al.* recently synthesized a DyLight750 labeled affibody, which targets HER2 receptor (ex/em: 754/776 nm), and demonstrated that the bioconjugate shows 150 ps higher FLT when bound to HER2 in tumor than when bound to non-tumor tissue mice.⁴⁹ The FLT of fluorescent Hilyte Fluor 488 (ex/em: 497/525 nm) conjugates of amyloid β (A β) peptides were shown to decrease from 3.7 ns in monomeric form to <3.3 ns upon aggregation. This feature was used to study the kinetics of cellular amyloid formation, which is implicated in Alzheimer's disease.⁵⁰ With the aid of super-resolution microscopy and FLIM methodology, the study showed good correlation of the observed dye FLT with the shape and size of the A β aggregates *in situ*.

Some fluorescent cell permeable drugs such as doxorubicin (ex/em: 470/530 nm) intercalate with DNA, transforming its FLT from ~1.1 ns in free form to ~2.4 ns when bound to DNA.⁵¹ Because this anticancer drug exerts its therapeutic effect in the nucleus, FLT mapping could be used to determine the therapeutic component of the internalized drug concentration. Changes in FLT based on biomolecular interactions could improve the information content available to scientists in the local tissue environment of interest. Not only can this approach be used to localize tumors, for example, it could also report the response to treatment by depletion of a target protein known to alter the molecular probe's FLT.

3.2.2. Biochemical Environment-Responsive FLT Molecular Probes—The biochemical compositions of cells and tissues of living organism are tightly controlled to achieve homeostasis, but pathologic conditions can significantly alter the concentrations of various ions and electrolytes. As a result, a variety of detection schemes have been developed to determine concentration and distribution of these biochemicals in cells and living systems. Although FLT imaging studies in this area are limited, we highlight below some studies of interest that are expected to grow in the future.

3.2.2.1. Acid-Responsive FLT Molecular Imaging Probes: Significant deviation of normal pH of cellular organelles and the extracellular space leads to, or results from a host of pathologic conditions, including cancer. Consequently, concerted efforts to determine this physiologic parameter have increased recently. Many organic fluorophores containing oxygen or nitrogen as part of the fluorophore system exhibit changes in fluorescence intensity or emission wavelength at different pH values. However, the FLT approach provides a versatile method to determine pH values in cells and tissue. Typically, protonation of the fluorophore could produce different fluorescent states of the molecule, leading to different fluorescent lifetimes. Thus, mapping of the pH of cells and tissue can be obtained by measuring pH-induced changes in the fractional contribution of each component to the average FLT. Unfortunately, the FLT of many fluorophore systems does not respond in the physiological relevant pH region (pH = 4.8–7.4).⁴ Representative examples of widely used FLT sensors of pH include (2',7'-Bis-(2-Carboxyethyl)-5-(and-6)-Carboxyfluorescein, a fluorescein based indicator that exhibits significantly different FLTs of 2.75 and 3.9 ns at pH 4.5 and 8, respectively.⁵² The protonated and deprotonated states of fluorescent imidazoles (ex/em: 320-520/560-700 nm) possess two distinct FLT of 0.3 and 0.5 ns, respectively.⁵³ Similarly, the FLT of enhanced GFPs (EGFP; ex/em: 488/509 nm) is 2.4–3.0 ns at pH 7.5, which decreases to 1.0–1.7 ns at pH <5.6.⁵⁴ These fluorophore systems can therefore be used for ratiometric or direct readout of pH after appropriate calibration. The lower dependency of the FLT on fluorophore concentration minimizes errors that result from intensity variations associated with differences in fluorophore concentration rather than with differences in underlying local pH.

Acid-sensitive biodegradable near-infrared (NIR) fluorescent nanoparticles were recently synthesized and their stability in different acidic conditions were studied by FLT technique.⁵⁵ In the presence of BSA solution at pH 7, FLT of 0.36 ns constituting 93% fractional contribution was determined, which corresponds to the value of the free NIR dye in aqueous environment. The result indicated that the dye was not exposed to BSA, which typically increases its FLT, and that the interior of the nanoparticles was hydrophilic. Time-dependent measurement of the FLT under acidic condition (pH 4) showed the emergence of a second FLT of 0.98 ns with fractional contribution of 74%, demonstrating the hydrolysis of the acid labile linkages in the nanoparticles and the release of the sequestered dye molecules. The new FLT corresponds to the BSA-bound NIR dye used in this study. Computing the ratio of the 0.36 and 0.96 ns FLTs facilitates the determination of degradation rate under diverse acidic conditions. To optimize biological imaging of pH using FLT method, new pH-sensitive NIR FLT molecular probe LS482 (ex/em: 700/715-950 nm; Figure 3)⁵⁶ with pKa ~5.5 was developed. The molecular probe delivers steady-state FLT pH-sensitivity with two distinct FLT for protonated (~1.16 ns in acidic DMSO) and deprotonated (~1.4 ns in basic DMSO) components.⁵⁶ See Figure 3 for more details.

Many organic fluorophore systems possess short FLTs that fall within the regime of endogenous fluorophore FLTs. In addition, the FLTs of organic fluorophores also have very small dynamic ranges, requiring high temporal resolution and sophisticated software to extract information from small FLT changes in heterogeneous media such as cells and thick

tissue. To enhance FLT application in cells and living organisms, inorganic nanoparticles possessing long FLTs, such as quantum dots (QDs), have been explored. Although long FLT is desirable, the associated long acquisition time will be less practical for imaging molecular processes on reasonable time scale. A recent study showed that modulation of CdTeSe/ZnS QDs (ex/em: 488/750 nm) FLT with a pH-sensitive NIR organic carbocyanine dye LS662 could increase the FLT dynamic range for pH sensing.⁵⁷ FLT of the hybrid nanoconstruct ranged from 29 ns at pH >7 to 12 ns at pH <5.

The FLT technique was recently used to image intracellular pH.⁵⁸ The FLT of mercaptopropionic acid-capped QDs (ex/em: 440/535 nm) varied from 8.7 ns (pH <5) to 15.4 ns (pH >8).⁵⁸ Using FLIM, Aigner *et al.* demonstrated the distribution of pH sensitive anionic perylene bisimide encapsulated in cationic nanoparticles (ex/em: 550/600 nm) in cells,⁵⁹ with predictable FLT changes from 4.7 to 3.7 ns between pH 4.4 and 8. Similarly, Carlini *et al.* reported the local pH in cellular organelles using pH sensitive CdSe-ZnS QDs or a dopamine-QD conjugates (ex/em: 570/580 nm).⁶⁰ Distinct FLTs were reported in different cellular organelles. The FLTs of cells treated with CdSe-ZnS QDs were 1.7, 6.6, and 2.3 ns in the endosome, cell membrane, and cytoplasm, respectively. Similarly, different FLTs of 1.2 ns, 2.9 ns, and 2.3 ns were found in cells treated with QD-dopamine conjugates in the same respective organelles, but the trend was the same in both cases (Figure 4).

The ensemble of these studies demonstrate the high potential of using FLT reporting strategy to elucidate pH-mediated molecular events. As the calibration curves for these molecular probes become more reliable in cells and tissue, it is anticipated that FLT measurements will become an important imaging technique for interrogating diverse cellular and pathophysiological processes in future.

3.2.2.2. Electrolyte-Responsive FLT Molecular Imaging Probes: In addition to hydrogen ions discussed above, the FLT technique is widely used to determine the presence or concentration of many biologically useful electrolytes. In most molecular probes, binding of the ions to the fluorophore systems induces a significant change in the FLT, which can provide an excellent FLT map of physiological processes. For example, the binding of chloride ions to N-(ethoxycarbonylmethyl)-6-methoxyquinolinium bromide (MQAE; ex/em: 355/460 nm) decreases the molecular probe's FLT from 5.9 ns to 3.4 ns and this information has been used to study the salivary glands of cockroaches (Figure 5).⁶¹ Similarly, the selective binding of calcium and sodium ions to Oregon Green BAPTA-1 (ex/em: 494/523 nm)⁶² and Sodium Green (ex/em: 506/532 nm),⁶³ respectively, generates distinct FLT changes for mapping signal activation or biological activity. Other molecular probes such as a monoboronic acid-naphthalimide derivative (ex/em: 465/525 nm)⁶⁴ and thieno-imidazole based polymer (ex/em: 375/390 nm)⁶⁵ have been developed for detecting copper and zinc, respectively. The FLTs of these molecular probes range from ~0.5 to ~10 ns. Short FLTs are important for imaging physiological processes of short duration. The potential to multiplex information is pertinent here because many of the sensors emit light within similar spectral range, but have distinct FLTs. Conceivably, imaging the distribution of multiple electrolytes in a region of interest could shed light on the spatio-temporal interactions between the ions as a function of specific biological activity.

3.2.2.3. Oxygen Species-Responsive Phosphorescence Lifetime Molecular Imaging

Probes: Oxygen and its derivatives play an important role in the normal functioning of the body. Certain molecules can emit phosphorescence following electronic transition from singlet to triplet states via intersystem crossing. Phosphorescent molecules are characterized by long excited triplet state lifetime, ranging from 500 ns to hundreds of microseconds. Perturbation of the long-lived lifetime by oxygen species has been used to monitor tissue oxygenation. For example, significant changes in the phosphorescence lifetime of ruthenium complexes (ex/em: 510-580/702-807 nm),⁶⁶ pyrenes (ex/em: 336/380 nm),⁶⁷ palladium(II)-meso-tetraphenyltetraabenzoporphyrin in O₂-permeable poly(styrene-co-acrylonitrile) microparticles (ex/em: 444/797 nm),⁶⁸ and mitoImageTM-NanO₂ and mitoImageTM-MM2 (ex/em: 405/650 nm) upon interaction with molecular oxygen have been used to image oxygen distribution and tissue hypoxia.⁶⁹ The phosphorescence lifetime of these molecular probes Lanthanide complexes (ex/em: 310-400/500-750 nm) have been used to determine singlet oxygen *via* phosphorescence lifetime imaging.⁷⁰ Some specialty molecular probes have been developed for photoluminescence lifetime imaging of hydrogen peroxide and nitric oxide.^{71, 72} Cellular and tissue lifetime imaging of these species is still evolving, and progress will benefit from the development of molecular probes that respond rapidly and specifically to oxygenation changes or the presence of high levels of reactive oxygen species and free radicals in heterogeneous mediums.

3.2.3. Physical Environment-Responsive FLT Molecular Probes—Several physical factors can alter the FLT of molecular probes. When these changes are predictable and reproducible, FLT imaging can report the status of these factors in cells and tissue. We summarize below a few studies that used FLT technique to determine the physical microenvironment of cells.

3.2.3.1. Temperature-Responsive FLT Molecular Imaging Probes: Molecular probes with rotatable group typically serve as FLT sensors of local temperature. For example, the increased rotational motion of a freely rotatable N-ethylenic group in the dye Rhodamine-B (ex/em: 540/625 nm) leads to high non-radiative decay at elevated temperature. Reproducible decrease in the FLT of this molecular probe from ~2.25 ns at 10 °C to ~0.25 ns at 95 °C was observed.⁷³ Application of FLT to image intracellular temperature was recently demonstrated using a fluorescent polymeric thermometer (ex/em: 456/565 nm).⁷⁴ Changing the temperature of the cellular medium from 28 °C to 40 °C increased the FLT from 4 ns to 7.5 ns, while maintaining excellent 0.18-0.58 °C temperature resolution at 200 nm spatial resolution in cells (Figure 6). This imaging platform could become useful for guiding the thermal treatment of diseases such as cancer and for monitoring tissue metabolism in resting state or after exercise.

3.2.3.2. Viscosity-Responsive FLT Molecular Imaging Probes: The intracellular microenvironment is highly heterogeneous, as reflected by differences in the viscosity of various compartments, ranging from the more fluidic cytosol to the highly viscous membranes. A special class of fluorescent molecules known as molecular rotors is widely used to determine the viscosity of biological mediums.⁷⁵ Upon absorption of light, these fluorophores can decay by a conventional S₁ to S₀ fluorescence pathway or undergo non-

radiative intramolecular twisting, which leads to a decrease in fluorescence. As the medium becomes more viscous, fluorescence instead of intramolecular rotation becomes the preferred deactivation pathway for the excited fluorophore, leading to the enhancement of fluorescence intensity. By calibrating the change in fluorescence as a function of the medium viscosity, molecular rotors provide an excellent method to report viscosity of cellular compartments using fluorescence microscopy.⁷⁶ In addition to viscosity response, fluorescence intensity can be altered by changes in the fluorophore concentration, excitation light power, and light interaction with biomolecules. To minimize variability, quantitative viscosity measurements using intensity readouts have been achieved by using a ratiometric approach consisting of measuring the fluorescence of viscosity-insensitive dye and viscosity sensitive molecular rotor.⁷⁷ However, this approach requires the synthesis and conjugation of another fluorophore to the rotor, creating a new entity with different intracellular distribution and retention properties. In contrast, fluorescence lifetime measurement of molecular rotors allows performing quantitative viscosity measurement without encountering the inherent limitations of intensity technique or the need for complex synthesis of multi-fluorophore systems. Direct conjugation of the fluorophores to a biomolecule will suffice to interrogate diverse intracellular mediums. Example includes membrane FLT sensors, which have been developed based on viscosity response (Figure 7).⁷⁸ In another recent work, using a fluorescent photoinduced electron transfer process to alter the FLT of a molecular probe (ex/em: 370/550 nm), Liu *et al.* determined the cellular lysosomal and mitochondrial viscosities as 130-175 cP and 60-120 cP, respectively.⁷⁹ Additional information detailing the design and use of viscosity sensitive molecular probes for cellular imaging is available elsewhere.^{75, 80, 81, 82, 83}

4. FUTURE DIRECTIONS

Fluorescence intensity measurements will continue to be widely used for routine biological assays and imaging. However, the emergence of imaging systems that are capable of extracting FLT parameters from fluorescence data provides a new dimension in data analysis. As a complementary parameter, the FLT can provide functional information that may not be available from intensity measurements alone. Another exciting feature of FLT imaging is the potential to multiplex information using diverse molecular probes with similar excitation and emission spectra, but significantly different FLTs. Furthermore, biological events such as enzymatic activities or acidic pH environment could change fluorescence intensity at the same wavelength, making it difficult to delineate the effects of differences in the local concentration of the molecular probe from the functional status of the molecular target in tissue. By designing molecular probes that can transform to different fluorescent states, changes in the fractional contribution of each FLT to the average FLT could be used for functional imaging. A pressing problem is the limited availability of FLT responsive molecular probes for biological imaging. In particular, the trend toward deep tissue imaging with NIR light will benefit from the development of molecular probes with programmable FLTs in this region. To minimize interference from endogenous fluorophores, exogenous molecular probes with FLTs greater than 8 ns are preferred. However, very long FLTs will require long data acquisition time, which may not be suitable for interrogating biological activities on short time scales.

5. CONCLUSION

The past decade has seen unprecedented progress in the use of optical imaging to interrogate cellular processes and pathophysiologic conditions in cells and small animal models of human diseases. Efforts to translate these preclinical methods to human patients have increased. Although most of these methods rely on fluorescence intensity measurements, unique or complementary information can be derived from the intrinsic or exogenous FLT of fluorophores. Particularly, the lower dependence of FLT on the fluorophore concentration can minimize imaging artifacts and provide reproducible data over long imaging periods. In addition, the FLT of some molecular probes changes as a function of their microenvironment, facilitating their use to determine the impact of environmental factors in pathophysiology. As newer and intentionally designed molecular probes for sensing specific molecular processes become available, we expect an acceleration in the adoption of this technique in biological imaging. Similarly, molecular probes with distinct, but stable FLT are needed to realize the full potential of using FLT technique for information multiplexing. Although we did not discuss FLT instrumentation in this review, progress in FLT imaging platform strongly depends on the availability of imaging systems with high temporal resolution, fast data acquisition time and analysis, and high spatial resolution for both cellular and deep tissue imaging applications.

Acknowledgments

Some of the studies described in this review were supported by the National Institutes of Health (NIH) shared instrumentation grant (S10 OD016237), the Molecular Imaging Center funded by the NCI (P50CA094056), and a research grant funded by the NCI (R01 CA171651) and NIBIB (R01 EB008111). DM was supported by the Imaging Sciences Pathway graduate student fellowship, at Washington University in St. Louis, under grant number NIH T32 EB014855. The authors thank Dr. Nalinikanth Kotagiri for discussion on other static probes and future directions. Image of 4KW4 (T.J. Barnard, X. Yu, N. Noinaj, J.W. Taraska crystal structure of green fluorescent protein at 1.75 Å resolution, <http://www.rcsb.org/pdb/explore.do?structureId=4KW4>) created with Chem3D Pro 13.0 (Perkin Elmer) was used in the TOC artwork and Figure 1.

References

1. Lakowicz, JR. Principles of Fluorescence Spectroscopy. 2. Kluwer Academic/Plenum Publishers; New York: 1999.
2. Guilbault, GG. Practical Fluorescence. 2. CRC Press; 1990.
3. Nothdurft RE, Patwardhan SV, Akers W, Ye YP, Achilefu S, Culver JP. In vivo fluorescence lifetime tomography. *J Biomed Opt.* 2009; 14
4. Berezin MY, Achilefu S. Fluorescence lifetime measurements and biological imaging. *Chem Rev (Washington, DC, U S).* 2010; 110:2641–2684.
5. Monici M. Cell and tissue autofluorescence research and diagnostic applications. *Biotechnol Ann Rev.* 2005; 11:227–56. [PubMed: 16216779]
6. Elson D, Requejo-Isidro J, Munro I, Reavell F, Siegel J, Suhling K, Tadrous P, Benninger R, Lanigan P, McGinty J, et al. Time-domain fluorescence lifetime imaging applied to biological tissue. *Photochem Photobiol Sci.* 2004; 3:795–801. [PubMed: 15295637]
7. Jo JA, Fang Q, Papaioannou T, Baker JD, Dorafshar AH, Reil T, Qiao JH, Fishbein MC, Freischlag JA, Marcu L. Laguerre-based method for analysis of time-resolved fluorescence data: application to in-vivo characterization and diagnosis of atherosclerotic lesions. *J Biomed Opt.* 2006; 11:021004. [PubMed: 16674179]
8. Butte PV, Mamelak AN, Nuno M, Bannykh SI, Black KL, Marcu L. Fluorescence lifetime spectroscopy for guided therapy of brain tumors. *NeuroImage.* 2011; 54(Suppl 1):S125–35. [PubMed: 21055475]

9. McGinty J, Galletly NP, Dunsby C, Munro I, Elson DS, Requejo-Isidro J, Cohen P, Ahmad R, Forsyth A, Thillainayagam AV, et al. Wide-field fluorescence lifetime imaging of cancer. *Biomed Opt Express*. 2010; 1:627–640. [PubMed: 21258496]
10. Cicchi R, Crisci A, Cosci A, Nesi G, Kapsokalyvas D, Giancane S, Carini M, Pavone FS. Time- and Spectral-resolved two-photon imaging of healthy bladder mucosa and carcinoma in situ. *Opt Express*. 2010; 18:3840–9. [PubMed: 20389394]
11. Gallas JM, Eisner M. Fluorescence of melanin-dependence upon excitation wavelength and concentration. *Photochem Photobiol*. 1987; 45:595–600.
12. De Giorgi V, Massi D, Sestini S, Cicchi R, Pavone FS, Lotti T. Combined non-linear laser imaging (two-photon excitation fluorescence microscopy, fluorescence lifetime imaging microscopy, multispectral multiphoton microscopy) in cutaneous tumours: first experiences. *Journal of the European Academy of Dermatology and Venereology : JEADV*. 2009; 23:314–6. [PubMed: 19207664]
13. Patalay R, Talbot C, Alexandrov Y, Munro I, Neil MA, Konig K, French PM, Chu A, Stamp GW, Dunsby C. Quantification of cellular autofluorescence of human skin using multiphoton tomography and fluorescence lifetime imaging in two spectral detection channels. *Biomed Opt Express*. 2011; 2:3295–308. [PubMed: 22162820]
14. Dimitrow E, Riemann I, Ehlers A, Koehler MJ, Norgauer J, Elsner P, Konig K, Kaatz M. Spectral fluorescence lifetime detection and selective melanin imaging by multiphoton laser tomography for melanoma diagnosis. *Exp Dermatol*. 2009; 18:509–15. [PubMed: 19243426]
15. Miura Y, Huettmann G, Orzekowsky-Schroeder R, Steven P, Szaszak M, Koop N, Brinkmann R. Two-photon microscopy and fluorescence lifetime imaging of retinal pigment epithelial cells under oxidative stress. *Invest Ophthalmol Vis Sci*. 2013; 54:3366–77.
16. Ying W. NAD⁺/NADH and NADP⁺/NADPH in cellular functions and cell death: regulation and biological consequences. *Antioxid Redox Signaling*. 2008; 10:179–206.
17. Gafni A, Brand L. Fluorescence decay studies of reduced nicotinamide adenine dinucleotide in solution and bound to liver alcohol dehydrogenase. *Biochemistry*. 1976; 15:3165–71. [PubMed: 8086]
18. Maeda-Yorita K, Aki K. Effect of nicotinamide adenine dinucleotide on the oxidation-reduction potentials of lipoamide dehydrogenase from pig heart. *J Biochem*. 1984; 96:683–90. [PubMed: 6548741]
19. Skala MC, Richtig KM, Gendron-Fitzpatrick A, Eickhoff J, Eliceiri KW, White JG, Ramanujam N. In vivo multiphoton microscopy of NADH and FAD redox states, fluorescence lifetimes, and cellular morphology in precancerous epithelia. *Proc Natl Acad Sci U S A*. 2007; 104:19494–9. [PubMed: 18042710]
20. Cicchi R, Massi D, Sestini S, Carli P, De Giorgi V, Lotti T, Pavone FS. Multidimensional nonlinear laser imaging of Basal Cell Carcinoma. *Opt Express*. 2007; 15:10135–48. [PubMed: 19547362]
21. Cicchi R, Pavone FS. Non-linear fluorescence lifetime imaging of biological tissues. *Anal Bioanal Chem*. 2011; 400:2687–97. [PubMed: 21455652]
22. Thompson AJ, Coda S, Sorensen MB, Kennedy G, Patalay R, Waitong-Bramming U, De Beule PA, Neil MA, Andersson-Engels S, Bendsoe N, et al. In vivo measurements of diffuse reflectance and time-resolved autofluorescence emission spectra of basal cell carcinomas. *J Biophotonics*. 2012; 5:240–54. [PubMed: 22308093]
23. Coda S, Thompson AJ, Kennedy GT, Roche KL, Ayaru L, Bansi DS, Stamp GW, Thillainayagam AV, French PM, Dunsby C. Fluorescence lifetime spectroscopy of tissue autofluorescence in normal and diseased colon measured ex vivo using a fiber-optic probe. *Biomed Opt Express*. 2014; 5:515–38. [PubMed: 24575345]
24. Sun Y, Hatami N, Yee M, Phipps J, Elson DS, Gorin F, Schrot RJ, Marcu L. Fluorescence lifetime imaging microscopy for brain tumor image-guided surgery. *J Biomed Opt*. 2010; 15:056022. [PubMed: 21054116]
25. Lagarto J, Dyer BT, Talbot C, Sikkell MB, Peters NS, French PM, Lyon AR, Dunsby C. Application of time-resolved autofluorescence to label-free in vivo optical mapping of changes in

- tissue matrix and metabolism associated with myocardial infarction and heart failure. *Biomed Opt Express*. 2015; 6:324–46. [PubMed: 25780727]
26. Dougherty CA, Vaidyanathan S, Orr BG, Holl MMB. Fluorophore:Dendrimer Ratio Impacts Cellular Uptake and Intracellular Fluorescence Lifetime. *Bioconj Chem*. 2015; 26:304–315.
 27. Wu TJ, Tzeng YK, Chang WW, Cheng CA, Kuo Y, Chien CH, Chang HC, Yu J. Tracking the engraftment and regenerative capabilities of transplanted lung stem cells using fluorescent nanodiamonds. *Nat Nanotechnol*. 2013; 8:682–9. [PubMed: 23912062]
 28. Nothdurft R, Sarder P, Bloch S, Culver J, Achilefu S. Fluorescence lifetime imaging microscopy using near-infrared contrast agents. *J Microsc*. 2012; 247:202–7. [PubMed: 22788550]
 29. Hoffmann K, Behnke T, Grabolle M, Resch-Genger U. Nanoparticle-encapsulated vis- and NIR-emissive fluorophores with different fluorescence decay kinetics for lifetime multiplexing. *Anal Bioanal Chem*. 2014; 406:3315–22. [PubMed: 24429975]
 30. Kobayashi H, Ogawa M, Alford R, Choyke PL, Urano Y. New strategies for fluorescent probe design in medical diagnostic imaging. *Chem Rev (Washington, DC, U S)*. 2010; 110:2620–40.
 31. Yadav RB, Burgos P, Parker AW, Iadevaia V, Proud CG, Allen RA, O'Connell JP, Jeshtadi A, Stubbs CD, Botchway SW. mTOR direct interactions with Rheb-GTPase and raptor: sub-cellular localization using fluorescence lifetime imaging. *BMC Cell Biol*. 2013; 14:3. [PubMed: 23311891]
 32. Dore K, Labrecque S, Tardif C, De Koninck P. FRET-FLIM Investigation of PSD95-NMDA Receptor Interaction in Dendritic Spines; Control by Calpain, CaMKII and Src Family Kinase. *PLoS One*. 2014; 9:e112170. [PubMed: 25393018]
 33. Chen Y, Saulnier JL, Yellen G, Sabatini BL. A PKA activity sensor for quantitative analysis of endogenous GPCR signaling via 2-photon FRET-FLIM imaging. *Front Pharmacol*. 2014; 5:56. [PubMed: 24765076]
 34. Nobis M, McGhee EJ, Morton JP, Schwarz JP, Karim SA, Quinn J, Edward M, Campbell AD, McGarry LC, Evans TR, et al. Intravital FLIM-FRET imaging reveals dasatinib-induced spatial control of src in pancreatic cancer. *Cancer Res*. 2013; 73:4674–86. [PubMed: 23749641]
 35. Spoelgen R, Adams KW, Koker M, Thomas AV, Andersen OM, Hallett PJ, Bercery KK, Joyner DF, Deng M, Stoothoff WH, et al. Interaction of the apolipoprotein E receptors low density lipoprotein receptor-related protein and sorLA/LR11. *Neuroscience*. 2009; 158:1460–8. [PubMed: 19047013]
 36. Chen J, Miller A, Kirchmaier AL, Irudayaraj JM. Single-molecule tools elucidate H2A.Z nucleosome composition. *J Cell Sci*. 2012; 125:2954–64. [PubMed: 22393239]
 37. Kong A, Leboucher P, Leek R, Calleja V, Winter S, Harris A, Parker PJ, Larijani B. Prognostic value of an activation state marker for epidermal growth factor receptor in tissue microarrays of head and neck cancer. *Cancer Res*. 2006; 66:2834–43. [PubMed: 16510606]
 38. Abe K, Zhao L, Periasamy A, Intes X, Barroso M. Non-invasive in vivo imaging of near infrared-labeled transferrin in breast cancer cells and tumors using fluorescence lifetime FRET. *PLoS One*. 2013; 8:e80269. [PubMed: 24278268]
 39. Kokko T, Kokko L, Soukka T, Lövgren T. Homogeneous non-competitive bioaffinity assay based on fluorescence resonance energy transfer. *Anal Chim Acta*. 2007; 585:120–125. [PubMed: 17386655]
 40. Vuojola J, Lamminmäki U, Soukka T. Resonance Energy Transfer from Lanthanide Chelates to Overlapping and Nonoverlapping Fluorescent Protein Acceptors. *Anal Chem*. 2009; 81:5033–5038. [PubMed: 19438245]
 41. Becker W. Fluorescence lifetime imaging - techniques and applications. *J Microsc*. 2012; 247:119–136. [PubMed: 22621335]
 42. Zhang Z, Fan J, Cheney PP, Berezin MY, Edwards WB, Akers WJ, Shen D, Liang K, Culver JP, Achilefu S. Activatable molecular systems using homologous near-infrared fluorescent probes for monitoring enzyme activities in vitro, in cellulo, and in vivo. *Mol Pharm*. 2009; 6:416–27. [PubMed: 19718795]
 43. French T, So PTC, Weaver DJ, CoelhoSampaio T, Gratton E, Voss EW, Carrero J. Two-photon fluorescence lifetime imaging microscopy of macrophage-mediated antigen processing. *J Microsc*. 1997; 185:339–353. [PubMed: 9134740]

44. Goergen CJ, Chen HH, Bogdanov A, Sosnovik DE, Kumar AT. In vivo fluorescence lifetime detection of an activatable probe in infarcted myocardium. *J Biomed Opt.* 2012; 17:056001. [PubMed: 22612124]
45. Solomon M, Guo K, Sudlow GP, Berezin MY, Edwards WB, Achilefu S, Akers WJ. Detection of enzyme activity in orthotopic murine breast cancer by fluorescence lifetime imaging using a fluorescence resonance energy transfer-based molecular probe. *J Biomed Opt.* 2011; 16:066019. [PubMed: 21721820]
46. Alford R, Ogawa M, Hassan M, Gandjbakhche AH, Choyke PL, Kobayashi H. Fluorescence lifetime imaging of activatable target specific molecular probes. *Contrast Media Mol Imaging.* 2010; 5:1–8. [PubMed: 20101762]
47. Saxl T, Khan F, Matthews DR, Zhi ZL, Rolinski O, Ameer-Beg S, Pickup J. Fluorescence lifetime spectroscopy and imaging of nano-engineered glucose sensor microcapsules based on glucose/galactose-binding protein. *Biosens Bioelectron.* 2009; 24:3229–3234. [PubMed: 19442507]
48. Biffi S, Garrovo C, Macor P, Tripodo C, Zorzet S, Secco E, Tedesco F, Lorusso V. In Vivo Biodistribution and Lifetime Analysis of Cy5.5-Conjugated Rituximab in Mice Bearing Lymphoid Tumor Xenograft Using Time-Domain Near-Infrared Optical Imaging. *Mol Imaging.* 2008; 7:272–282. [PubMed: 19123997]
49. Ardeshirpour Y, Chernomordik V, Zielinski R, Capala J, Griffiths G, Vasalatiy O, Smirnov AV, Knutson JR, Lyakhov I, Achilefu S, et al. In vivo fluorescence lifetime imaging monitors binding of specific probes to cancer biomarkers. *PLoS One.* 2012; 7:e31881. [PubMed: 22384092]
50. Esbjorner EK, Chan F, Rees E, Erdelyi M, Luheshi LM, Bertocini CW, Kaminski CF, Dobson CM, Kaminski Schierle GS. Direct observations of amyloid beta self-assembly in live cells provide insights into differences in the kinetics of A β (1-40) and A β (1-42) aggregation. *Chem Biol.* 2014; 21:732–42. [PubMed: 24856820]
51. Chen NT, Wu CY, Chung CY, Hwu Y, Cheng SH, Mou CY, Lo LW. Probing the dynamics of doxorubicin-DNA intercalation during the initial activation of apoptosis by fluorescence lifetime imaging microscopy (FLIM). *PLoS One.* 2012; 7:e44947. [PubMed: 23028696]
52. Hille C, Berg M, Bressel L, Munzke D, Primus P, Lohmannsroben HG, Dosche C. Time-domain fluorescence lifetime imaging for intracellular pH sensing in living tissues. *Anal Bioanal Chem.* 2008; 391:1871–9. [PubMed: 18481048]
53. Berezin MY, Kao J, Achilefu S. pH-dependent optical properties of synthetic fluorescent imidazoles. *Chemistry.* 2009; 15:3560–6. [PubMed: 19212987]
54. Nakabayashi T, Wang HP, Kinjo M, Ohta N. Application of fluorescence lifetime imaging of enhanced green fluorescent protein to intracellular pH measurements. *Photochem Photobiol Sci.* 2008; 7:668–670. [PubMed: 18528549]
55. Almutairi A, Guillaudeu SJ, Berezin MY, Achilefu S, Frechet JM. Biodegradable pH-sensing dendritic nanoprobe for near-infrared fluorescence lifetime and intensity imaging. *J Am Chem Soc.* 2008; 130:444–445. [PubMed: 18088125]
56. Berezin MY, Guo K, Akers W, Northdurft RE, Culver JP, Teng B, Vasalatiy O, Barbacow K, Gandjbakhche A, Griffiths GL, et al. Near-infrared fluorescence lifetime pH-sensitive probes. *Biophys J.* 2011; 100:2063–72. [PubMed: 21504743]
57. Tang R, Lee H, Achilefu S. Induction of pH sensitivity on the fluorescence lifetime of quantum dots by NIR fluorescent dyes. *J Am Chem Soc.* 2012; 134:4545–8. [PubMed: 22360301]
58. Orte A, Alvarez-Pez JM, Ruedas-Rama MJ. Fluorescence lifetime imaging microscopy for the detection of intracellular pH with quantum dot nanosensors. *ACS Nano.* 2013; 7:6387–95. [PubMed: 23808971]
59. Aigner D, Dmitriev RI, Borisov SM, Papkovsky DB, Klimant I. pH-sensitive perylene bisimide probes for live cell fluorescence lifetime imaging. *J Mater Chem B.* 2014; 2:6792–6801.
60. Carlini L, Nadeau JL. Uptake and processing of semiconductor quantum dots in living cells studied by fluorescence lifetime imaging microscopy (FLIM). *Chem Commun (Cambridge, U K).* 2013; 49:1714–6.
61. Hille C, Lahn M, Lohmannsroben HG, Dosche C. Two-photon fluorescence lifetime imaging of intracellular chloride in cockroach salivary glands. *Photochem Photobiol Sci.* 2009; 8:319–327. [PubMed: 19255672]

62. Wilms CD, Eilers J. Photo-physical properties of Ca²⁺-indicator dyes suitable for two-photon fluorescence-lifetime recordings. *J Microsc.* 2007; 225:209–213. [PubMed: 17371443]
63. Despa S, Vecer J, Steels P, Ameloot M. Fluorescence lifetime microscopy of the Na⁺ indicator Sodium Green in HeLa cells. *Anal Biochem.* 2000; 281:159–75. [PubMed: 10870831]
64. Li M, Ge H, Arrowsmith RL, Mirabello V, Botchway SW, Zhu W, Pascu SI, James TD. Ditopic boronic acid and imine-based naphthalimide fluorescence sensor for copper(II). *Chem Commun (Cambridge, U K).* 2014; 50:11806–9.
65. Satapathy R, Wu YH, Lin HC. Novel thienoimidazole based probe for colorimetric detection of Hg²⁺ and fluorescence turn-on response of Zn²⁺ *Org Lett.* 2012; 14:2564–7. [PubMed: 22571681]
66. Hosny NA, Lee DA, Knight MM. Single photon counting fluorescence lifetime detection of pericellular oxygen concentrations. *J Biomed Opt.* 2012; 17:016007. [PubMed: 22352657]
67. Rharass T, Ribou AC, Vigo J, Salmon JM. Effect of Adriamycin treatment on the lifetime of pyrene butyric acid in single living cells. *Free Radical Res.* 2005; 39:581–588. [PubMed: 16036335]
68. Schreml S, Meier RJ, Kirschbaum M, Kong SC, Gehmert S, Felthaus O, Kuchler S, Sharpe JR, Woltje K, Weiss KT, et al. Luminescent dual sensors reveal extracellular pH-gradients and hypoxia on chronic wounds that disrupt epidermal repair. *Theranostics.* 2014; 4:721–35. [PubMed: 24883122]
69. Dmitriev RI, Zhdanov AV, Nolan YM, Papkovsky DB. Imaging of neurosphere oxygenation with phosphorescent probes. *Biomaterials.* 2013; 34:9307–17. [PubMed: 24016849]
70. Song B, Wang GL, Tan MQ, Yuan JL. A europium(III) complex as an efficient singlet oxygen luminescence probe. *J Am Chem Soc.* 2006; 128:13442–13450. [PubMed: 17031957]
71. Guo H, Aleyasin H, Dickinson BC, Haskew-Layton RE, Ratan RR. Recent advances in hydrogen peroxide imaging for biological applications. *Cell Biosci.* 2014; 4:64. [PubMed: 25400906]
72. Zhegalova NG, Gonzales G, Berezin MY. Synthesis of nitric oxide probes with fluorescence lifetime sensitivity. *Org Biomol Chem.* 2013; 11:8228–34. [PubMed: 24166035]
73. Benninger RKP, Koc Y, Hofmann O, Requejo-Isidro J, Neil MAA, French PMW, deMello AJ. Quantitative 3D mapping of fluidic temperatures within microchannel networks using fluorescence lifetime imaging. *Anal Chem.* 2006; 78:2272–2278. [PubMed: 16579608]
74. Okabe K, Inada N, Gota C, Harada Y, Funatsu T, Uchiyama S. Intracellular temperature mapping with a fluorescent polymeric thermometer and fluorescence lifetime imaging microscopy. *Nat Commun.* 2012; 3:705. [PubMed: 22426226]
75. Kuimova MK. Mapping viscosity in cells using molecular rotors. *Phys Chem Chem Phys.* 2012; 14:12671–86. [PubMed: 22806312]
76. Loison P, Hosny NA, Gervais P, Champion D, Kuimova MK, Perrier-Cornet JM. Direct investigation of viscosity of an atypical inner membrane of *Bacillus* spores: A molecular rotor/FLIM study. *Biochim Biophys Acta, Biomembr.* 2013; 1828:2436–2443.
77. Lubyphelps K, Mujumdar S, Mujumdar RB, Ernst LA, Galbraith W, Waggoner AS. A Novel Fluorescence Ratiometric Method Confirms the Low Solvent Viscosity of the Cytoplasm. *Biophys J.* 1993; 65:236–242. [PubMed: 8369435]
78. Kwiatek JM, Owen DM, Abu-Siniyeh A, Yan P, Loew LM, Gaus K. Characterization of a new series of fluorescent probes for imaging membrane order. *PLoS One.* 2013; 8:e52960. [PubMed: 23390489]
79. Liu T, Liu X, Spring DR, Qian X, Cui J, Xu Z. Quantitatively mapping cellular viscosity with detailed organelle information via a designed PET fluorescent probe. *Scientific reports.* 2014; 4:5418. [PubMed: 24957323]
80. Bastos, AEP.; Scolari, S.; Stöckl, M.; de Almeida, RFM. Chapter Three - Applications of Fluorescence Lifetime Spectroscopy and Imaging to Lipid Domains In Vivo. In: conn, PM., editor. *Methods Enzymol.* Academic Press; 2012. p. 57-81.
81. Kuimova MK, Yahioglu G, Levitt JA, Suhling K. Molecular rotor measures viscosity of live cells via fluorescence lifetime imaging. *J Am Chem Soc.* 2008; 130:6672–3. [PubMed: 18457396]

82. Levitt JA, Kuimova MK, Yahioglu G, Chung PH, Suhling K, Phillips D. Membrane-Bound Molecular Rotors Measure Viscosity in Live Cells via Fluorescence Lifetime Imaging. *J Phys Chem C*. 2009; 113:11634–11642.
83. Dora Tang TY, Rohaida Che Hak C, Thompson AJ, Kuimova MK, Williams DS, Perriman AW, Mann S. Fatty acid membrane assembly on coacervate microdroplets as a step towards a hybrid protocell model. *Nat Chem*. 2014; 6:527–533. [PubMed: 24848239]

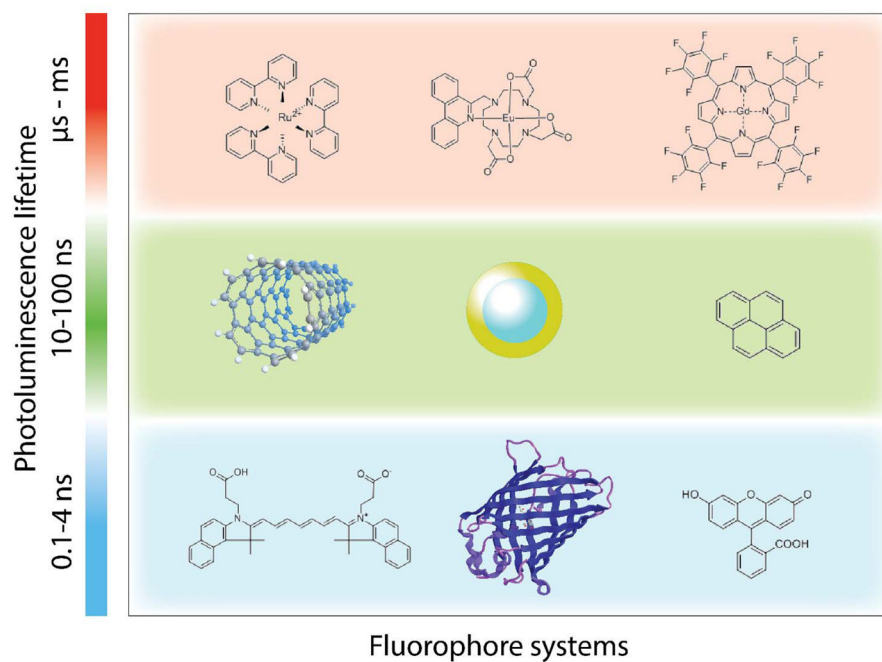


Figure 1. Representative fluorophore systems commonly used in lifetime imaging and associated photoluminescence lifetimes. These fluorophores can be used in their native forms and/or after conjugation to other entities.

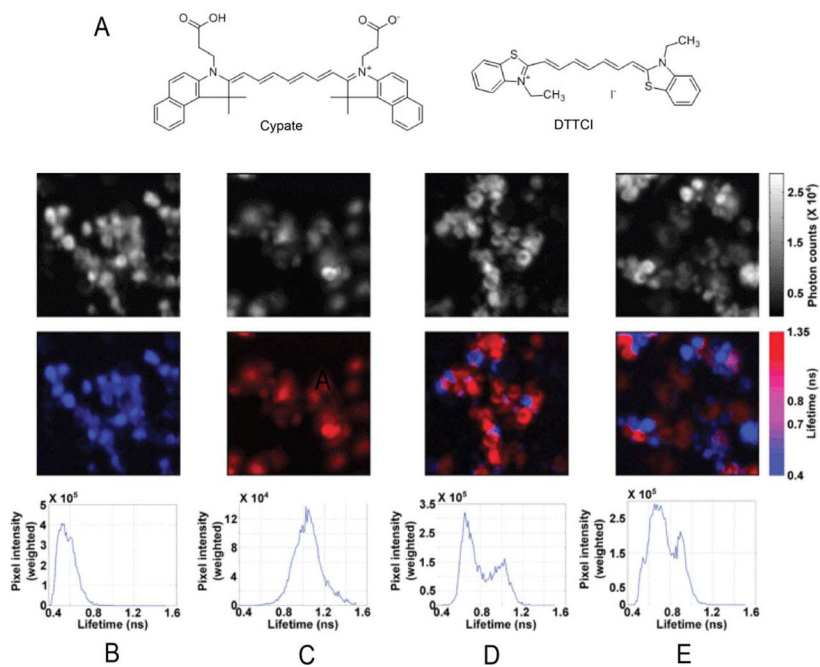


Figure 2.

(A) Structures of the NIR dyes cypate (ex/em: 792/810 nm) and 3,3'-diethylthiatricyanine iodide (DTTCI; ex/em: 771/800 nm) used in this study. (B) Intensity images (top row), FLIM images (middle row), and FLT distributions (bottom row) of cells treated with cypate alone. (C) Intensity images (top row), FLIM images (middle row), and FLT distributions (bottom row) of cells treated with DTTCI alone. (D) Intensity images (top row), FLIM images (middle row), and FLT distributions (bottom row) of cells treated with either cypate or DTTCI. (E) Intensity images (top row), FLIM images (middle row), and FLT distributions (bottom row) of cells treated with both cypate and DTTCI. Reprinted with permission from ref 28. Copyright 2012 Royal Microscopical Society.

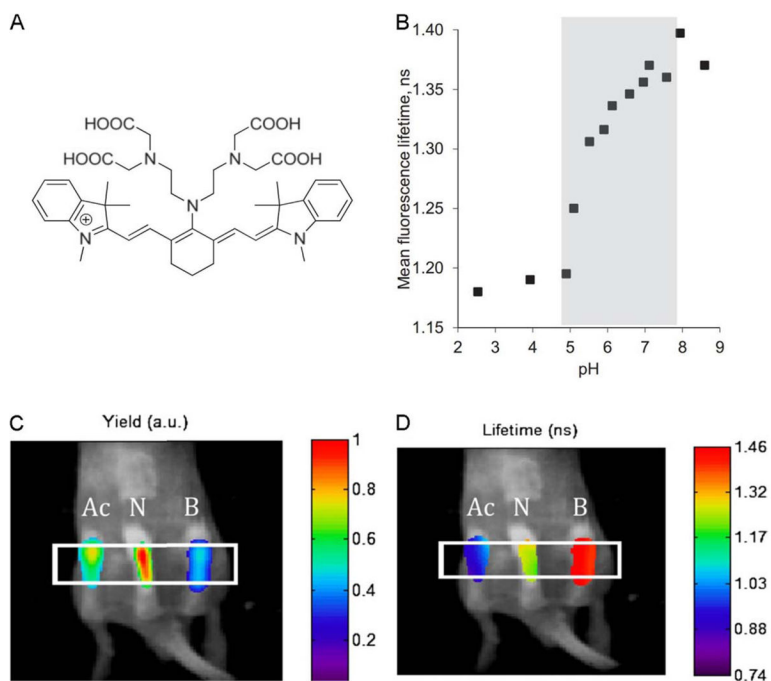


Figure 3. (A) Structure of LS482. (B) Spectroscopic FLT vs pH; $pK_a = 5.39$. (C, D) FLT tomography imaging of three phantoms (Ac, acidic; N, neutral; and B, basic) implanted into a mouse. A vertical slice from the tomography reconstructed yield (C) and lifetime (D) is overlaid on a white-light image of the mouse. (Reprinted from *Biophysical Journal*, vol. 100, no. 8, Berezin et al., Near-infrared fluorescence lifetime pH-sensitive probes, pp. 2063-72, Copyright (2011), with permission from Elsevier.)

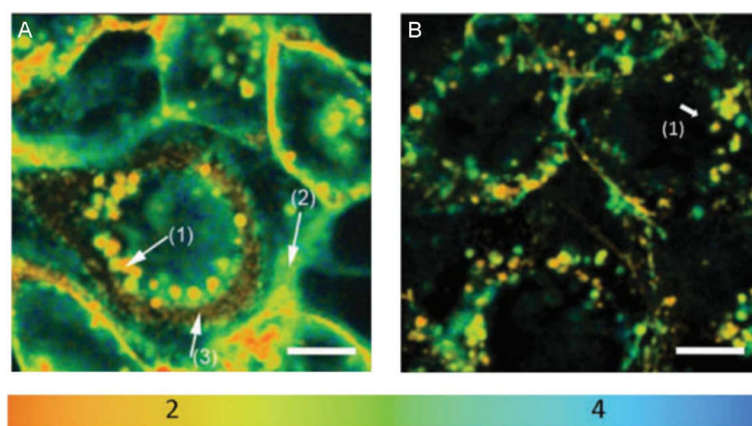


Figure 4. FLT images of (A) CdSe–ZnS and (B) CdSe–ZnS:dopamine QDs incubated with NIH 3T3 fibroblast cells. The color scale represents the lifetimes in ns; white scale bars are 10 μm. Note the inhomogeneous distribution of lifetimes in cells incubated with QD:dopamine conjugates compared to the structured lifetime distribution in cells incubated with QDs alone. Information on arrows is available in the original article. (Reproduced from the article by Carlini *et al.*,⁶⁰ with permission of The Royal Society of Chemistry. DOI: <http://dx.doi.org/10.1039/C3CC36326K>.)

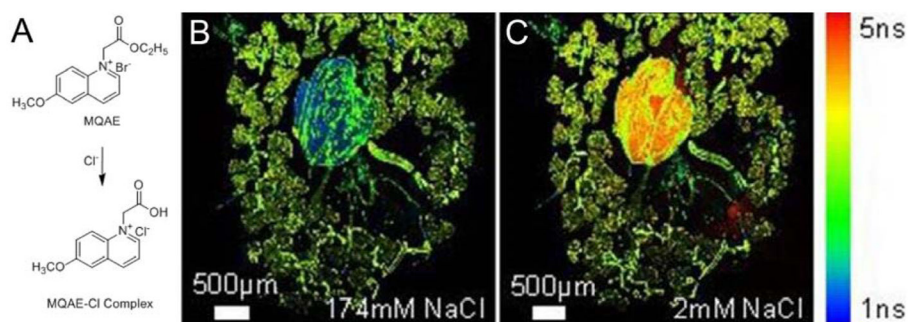


Figure 5. (A) Structure of MQAE and its Cl^- bound form. Dissected salivary glands of a cockroach, labeled with MQAE and placed in buffers with 174 mM NaCl (B) and 2 mM NaCl (C). (Courtesy of Carsten Hille, Physical Chemistry group, University of Potsdam.)

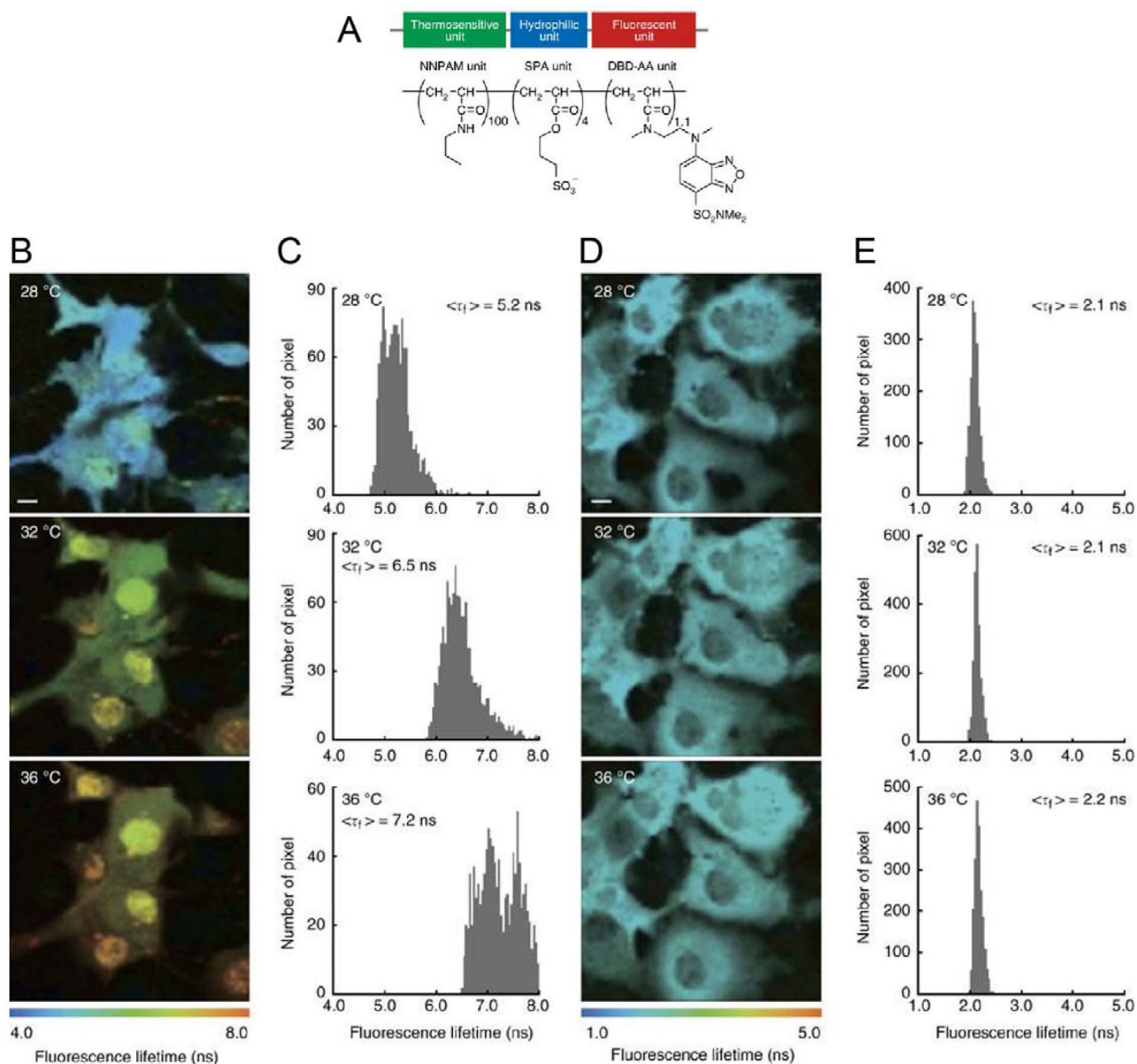
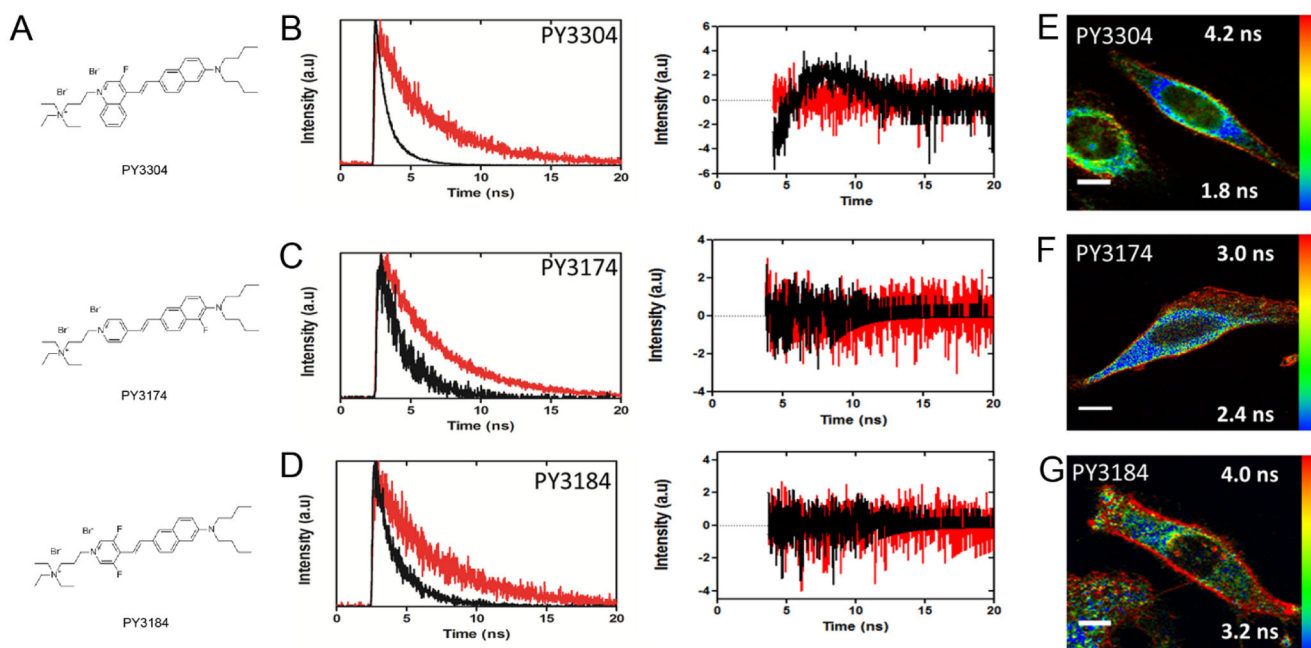


Figure 6.

Figure 6. (A) Chemical structure of fluorescent polymeric thermosensitive probe. (B) FLT images of the fluorescent polymeric thermometer in live cells. (C) Histograms of FLT derived from the cells. (D) FLT images of the control copolymer in live cells. (E) Histograms of FLT derived from the control cells. $\langle \tau_f \rangle$ represents an average lifetime of the histogram. Scale bar represents 10 μm . Reprinted with permission from Okabe et al.⁷⁴ Copyright 2012 Macmillan Publishers Ltd.

**Figure 7.**

(A) Structure of the viscosity-sensitive probes PY3304, PY3174, and PY3184. (B) Left: Fluorescence decays acquired from artificial membranes stained with PY3304 showing longer lifetimes in ordered membranes (red) than in disordered membranes (black). (Right) Plots of residuals from fitting fluorescence decays. (C) Fluorescence decays and plots of residuals from artificial membranes stained with PY3174 (D) Fluorescence decays and plots of residuals from artificial membranes stained with PY3184. (E) FLT image of live HeLa cells stained with PY3304 (F) FLT image of live HeLa cells stained with PY3174 (G) FLT image of live HeLa cells stained with PY3184. FLT images show an increased order at the plasma membrane. Scale bar = 10 μm . Reprinted from ref 78.